photooxidation of the imino groups—eq 2, can be related to the reactivity of an excited state with charge-transfer character, $CT_{\pi\text{-imino}\rightarrow\text{d-Ni}}$.

The photochemistries of the Ni(III) complexes contrast with that of the isoelectronic Co(II) species.[26] Indeed, the primary photochemical process of $Co([14]dieneN_4)^{2+}$ is determined by population of a metal to ligand, $CT_{\text{d-Co}\rightarrow{}^*\pi\text{-imino}}$, charge-transfer state. The differences that exist between the photochemistries of these isoelectronic systems might be related to the distinct accessibility of the oxidation states, a tripositive cobalt and a dipositive nickel.[2] A large unfavorable energy must be associated with the generation of a metal to ligand charge-transfer state, $CT_{\text{d-Ni(III)}\rightarrow{}^*\pi\text{-imino}}$, in the Ni(III) complex.[27] Therefore, either such a state might be out of the range of the excitation energies used here or it can be efficiently depopulated toward underlying charge-transfer states.

Acknowledgment. The research described herein was supported by the Office of Basic Energy Sciences of the Department of Energy. This is Document No. NDRL-1999 from the Notre Dame Radiation Laboratory.

Registry No. $Ni([14]dieneN_4)(CH_3CN)_2^{3+}$, 71435-49-9; $Ni(tet\ \alpha)(CH_3CN)_2^{3+}$, 71484-74-7.

References and Notes

(1) D. C. Olson and J. Vasilevskis, *Inorg. Chem.*, **10**, 463 (1971).

(2) D. P. Rillema, J. F. Endicott, and E. Papaconstantinou, *Inorg. Chem.*, **10**, 1739 (1971).

(3) J. C. Dabrowiak, F. Lovecchio, V. L. Goedken, and D. H. Busch, *J. Am. Chem. Soc.*, **94**, 5502 (1972).

(4) D. C. Olson and J. Vasilevskis, *Inorg. Chem.*, **8**, 1611 (1969).

(5) F. V. Lovecchio, E. S. Gore, and D. H. Busch, *J. Am. Chem. Soc.*, **96**, 3109 (1974).

(6) N. F. Curtis, *Coord. Chem. Rev.*, **3**, 3 (1968).

(7) E. K. Barefield and D. H. Busch, *Inorg. Chem.*, **10**, 108 (1971).

(8) V. L. Goedken and D. H. Busch, *J. Am. Chem. Soc.*, **94**, 7355 (1972).

(9) C. Hipp and D. H. Busch, *Inorg. Chem.*, **11**, 1988 (1972).

(10) V. L. Goedken and D. H. Busch, *Inorg. Chem.*, **10**, 2679 (1971).

(11) G. Ferraudi and L. K. Patterson, *J. Chem. Soc., Chem. Commun.*, 1955 (1977).

(12) P. Maruthamuthu, L. K. Patterson, and G. Ferraudi, *Inorg. Chem.*, **17**, 3157 (1978).

(13) M. Jaccobi, D. Meyerstein, and J. Lilie, *Inorg. Chem.*, **18**, 429 (1979).

(14) C. Hipp, L. F. Lindoy, and D. H. Busch, *Inorg. Chem.*, **11**, 1988 (1972).

(15) M. T. Mocella and E. K. Barefield, *Inorg. Chem.*, **12**, 2829 (1973).

(16) Ligand abbreviations: $[14]dieneN_4$, 5,7,7,12,14,14-hexamethyl-1,4,8,11-tetraazacyclotetradeca-4,11-diene; tet a, 5,7,7,12,14,14-hexamethyl-1,4,8,11-tetraazacyclotetradecane.

(17) G. Ferraudi, *Inorg. Chem.*, **17**, 1741 (1978).

(18) G. Ferraudi, *Inorg. Chem.*, **17**, 2506 (1978).

(19) G. Ferraudi and E. V. Srisankar, *Inorg. Chem.*, **17**, 3164 (1978).

(20) C. A. Parker and G. E. Hatchard, *Proc. R. Soc. London, Ser. A*, **518**, 1935 (1956).

(21) Notice that small amounts of either water or reducing impurities produce a rapid disappearance of the Ni(III) complexes.[4]

(22) The experimental error in these determinations and the yields for Ni(III) disappearance or Ni(II) formation give an upper limit for the yield of secondary photoreactions; $\phi \leq 2 \times 10^{-3}$.

(23) A significant anation of the $Ni([14]dieneN_4)(CH_3CN)_2^{3+}$ by sulfate ions is expected for concentrations of these species larger than those used here. Modifications of the absorption spectrum of $Ni([14]dieneN_4)(CH_3CN)_2^{3+}$, induced by sulfuric acid, reveal that the percentage of anated species must be equal to or smaller than 10%.

(24) C. K. Jørgensen, "Absorption Spectra and Chemical Bonding in Complexes", Addison-Wesley, Reading, Mass., 1962, pp 146–72.

(25) Notice that the disparity in the limiting yields can be attributed to differences between the efficiencies of interconversion to the reactive excited states, the lifetime of these states, and the rate constants of the redox processes in the excited state. However, some properties of the Ni(III) complexes[1-15] suggest that differences in the lifetimes of the charge-transfer states are more likely the reason for the distinct limiting yields.

(26) G. Ferraudi, *Inorg. Chim. Acta*, **34**, 274 (1979).

(27) The oxidation of Ni(III) to Ni(IV) has not been observed with nickel complexes of tet a and $[14]dieneN_4$.[2-4] However, the oxidation potentials of Co(II)/Co(III) couples show that oxidation of Co(II) to Co(III) in the field of the macrocycle is a more favorable process.[2,3]

Contribution from the Kenan Laboratories of Chemistry,
The University of North Carolina, Chapel Hill, North Carolina 27514

Chemical and Electrochemical Properties of 2,2'-Bipyridyl Complexes of Ruthenium Covalently Bound to Platinum Oxide Electrodes

H. D. ABRUÑA, THOMAS J. MEYER,* and ROYCE W. MURRAY*

Received February 6, 1979

The covalent attachment of 2,2'-bipyridyl complexes of ruthenium to silanized platinum oxide electrodes by two different surface synthetic procedures is demonstrated. The electrodes, once prepared, show an impressive stability toward cycling between the ruthenium(II) and -(III) oxidation states. The surface-attached complexes largely retain the chemical characteristics exhibited by their homogeneous solution analogues, but a quenching of photochemical behavior is observed. Although stable indefinitely in the Ru(II) state, once oxidized to Ru(III), the surfaces undergo a slow decay process which results ultimately in the complete loss of ruthenium from the surface. The surface decay processes have been found to follow first-order kinetics. Current–potential wave shapes for the surface-bound Ru(III)/Ru(II) couples are treated in the light of surface activity parameters.

Synthesis, structural and redox properties, and possible applications are all topics of current research on chemically modified electrodes.[1] Organosilane reagents form stable chemical bonds to the surfaces of metal oxide electrodes[2] including thin, anodically generated oxide films on platinum metal.[3] Other species can then be immobilized on the electrode surface by exploiting the chemical properties of the attached silane. We describe here the preparation and properties of platinum oxide surfaces bearing attached 2,2'-bipyridyl complexes of ruthenium.

One of the major themes of chemically modified electrode research is the transfer of chemical and electrochemical behavior of a reagent in homogeneous solution to the surface of an electrode. Catalytic reactions are of particular interest and attractiveness and, among homogeneous catalysts, many involve transition-metal complexes that exhibit a variety of stable oxidation states. Complexes of the type $[(bpy)_2Ru^{II}LL']$ (bpy is 2,2'-bipyridyl), as a rule, undergo reversible metal-localized $Ru^{II} \rightarrow Ru^{III}$ oxidations and bipyridyl-localized reductions.[4] Further, the potential for the $Ru^{III,II}$ couples can be systematically varied by ca. 1.5 V by an appropriate selection of the ligands L and L'.[4] In some cases, the excited states of the Ru^{II} complexes have been shown to have an extensive redox chemistry which could conceivably provide the basis for useful energy conversion processes.[5] In addition, recent work has shown that polypyridyl complexes of ruthenium can provide the basis for potentially useful oxidation catalysts in solution where the catalytic cycles are driven by electrochemical oxidation.[6]

Experimental Section

Electrode Pretreatment. Mirror-polished (1-μm diamond paste) Pt disk electrodes anodized for ca. 5 min at +1.9 V vs. SCE in 1 M H_2SO_4 were cycled between hydrogen and oxygen discharge until the characteristic clean Pt wave pattern was observed.[7] The electrodes were then potentiostated at +1.1 V for 2 min, washed thoroughly with distilled water, and vacuum-dried at 50 °C for 20 min. Electrode surface areas were determined by using a standard technique.[7]

Silanization. The dried electrodes were placed in serum-capped vials, the vials were flushed with dry N_2, and the electrodes were washed with dry toluene for ca. 5 min. After being washed, the electrodes were allowed to react, under positive N_2 pressure, with an anhydrous 8% toluene solution of [3-[(2-aminoethyl)amino]propyl]trimethoxysilane (en-silane) for 5 min. The silanized electrodes, designated Pt/PtO/en, were washed six times with dry toluene and then twice with the solvent to be used for the amidization reaction step. Silanization with 4-[β-trichlorosilyl)ethyl]pyridine (py-silane) involved an identical procedure except that the Pt/PtO electrodes were silanized for 8 min with a toluene extract of the py-silane reagent. These surfaces are designated Pt/PtO/py.

Attachment of Ruthenium Complexes. Table I gives, in summary form, the reaction conditions used to attach the various complexes. The concentrations of complex used in the experiments were generally in the range 1–3 mM.

Syntheses. [Ru(bpy)$_2$(*i*-nic)$_2$][PF$_6$]$_2$ (I; *i*-nic = Isonicotinic Acid, Pyridine-4-carboxylic Acid). The bis(isonicotinic acid) complex was prepared by heating at reflux for 8 h and under N_2 a deaerated aqueous solution containing *cis*-$Ru(bpy)_2Cl_2{\cdot}2H_2O$ and a tenfold molar excess of isonicotinic acid. The deep orange-red solution was cooled and filtered, and the complex was precipitated by addition of a saturated aqueous solution of NH_4PF_6. The solid was collected, washed three times with 5-mL portions of water and once with ether, and dried in a vacuum oven. The solid was purified by dissolving in a minimum quantity of acetone and reprecipitating with ether. The product was collected, washed with ether, and dried in a vacuum oven at 25 °C for 24 h. Anal. Calcd: C, 39.69; N, 8.68; H, 2.89. Found: C, 39.17; N, 8.77; H, 2.98.

Ru(bpy)$_2$(*i*-nic)Cl][PF$_6$] (II) was prepared by heating at reflux for 3 h and under N_2 a deaerated aqueous solution of *cis*-$Ru(bpy)_2Cl_2{\cdot}2H_2O$ containing a 20% molar excess of isonicotinic acid. The product was isolated and purified as for I. Anal. Calcd: C, 43.6; N, 9.77; H, 2.95. Found: C, 43.8; N, 9.76; H, 2.77.

Ru(bpy)$_2$(2,2′-bpy-4,4′-diacid)][PF$_6$]$_2$ (III) was prepared by heating for 8 h at reflux under N_2 a 1/1 (v/v) H_2O/ethanol solution of *cis*-$Ru(bpy)_2Cl_2{\cdot}2H_2O$ with a 20% molar excess of the bpy-diacid ligand. The bpy-diacid ligand was kindly provided by Dr. B. P. Sullivan. The product was isolated and purified as for I. Anal. Calcd: C, 38.28; N, 8.37; H, 2.70. Found: C, 38.05; N, 8.81; H, 2.71.

[Ru(bpy)$_2$(DME)]$^{2+}$ (IV). This complex was prepared by suspending *cis*-$Ru(bpy)_2Cl_2{\cdot}2H_2O$ (50–100 mg) in thoroughly deaerated dimethoxyethane[9] (25 mL) and adding a twofold excess of $AgPF_6$. The solution was stirred under N_2 at room temperature for 2 h. The precipitated AgCl was separated by filtration under N_2 and the solution used immediately. Subsequent work has shown that the reactant solutions at this point probably contain considerable amounts of $[Ru(bpy)_2(DME)Cl]^+$ and possibly some unprecipitated AgCl in addition to the chelated dimethoxyethane complex.

Reagents. Solvents. Spectrograde acetonitrile and reagent grade methylene chloride were dried over 4-Å molecular sieves. Reagent grade toluene was dried over sodium. Dimethoxyethane was purified by distillation from $LiAlH_4$. All other solvents were of at least reagent grade quality and were used without further purification.

Silanes. (a) [3-[(2-Aminoethyl)amino]propyl]trimethoxysilane ($(CH_3O)_3Si(CH_2)_3NH(CH_2)_2NH_2$, en-silane) (PCR or Petrarch) was vacuum distilled twice and stored in a desiccator. The material was vacuum distilled again immediately prior to use.

(b) 4-[β-(Trichlorosilyl)ethyl]pyridine ($Cl_3Si(CH_2)_2C_5H_4N$, py-silane) (Petrarch), used as received, was stored and handled inside a glovebox. Recently, this reagent became available as a 25% solution in toluene which we have handled in a similar fashion.

Instruments. X-ray photoelectron spectra (XPS) were taken with a Du Pont 650B electron spectrometer.[2a] Electrochemical cells and apparatus were conventional. All electrochemical experiments were done in dry acetonitrile with 0.1 M $[NEt_4][ClO_4]$ (TEAP) electrolyte. All potentials are referenced to the NaCl-saturated SCE (SSCE). The scan rate in all cyclic voltammetric experiments was 200 mV/s unless specified otherwise.

Results and Discussion

Attachment Chemistry. Two different synthetic strategies were used to attach the ruthenium complexes to the silanized platinum oxide surfaces. The chemical steps involved are shown in outline form in Scheme I, with examples of both procedures. In the first procedure the substitution-inert complexes I–III, which have exposed carboxylic acid groups, were first isolated and characterized as PF_6^- salts. The salts were then dissolved in an appropriate solvent (CH_2Cl_2 or CH_3CN) and allowed to react with the en-silanized electrodes in the presence of DDC, dicyclohexylcarbodiimide.[10] The carbodiimide is a dehydrating agent which assists the amide-coupling reaction between the carboxylic acid and the en-silane terminal amine group, by removing water as it is formed.

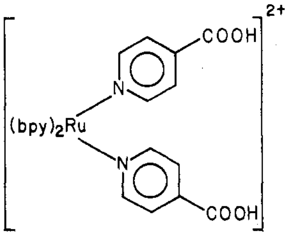
I, $[Ru(bpy)_2(i\text{-nic})_2]^{2+}$

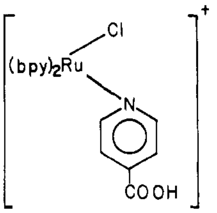
II, $[Ru(bpy)_2(i\text{-nic})Cl]^+$

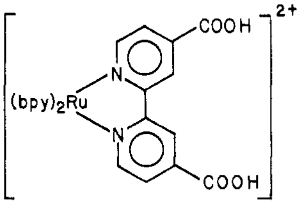
III, $[Ru(bpy)_2(bpy\text{-diacid})]^{2+}$

Scheme I

Procedure 1 (en-Silane Surface)

$$Pt/PtO + (CH_3O)_3Si(CH_2)_3NH(CH_2)_2NH_2 \rightarrow Pt/PtO/Si(CH_2)_3NH(CH_2)_2NH_2$$

$$Pt/PtO/Si(CH_2)_3NH(CH_2)_2NH_2 + [Ru(bpy)_2(4\text{-}pyCO_2H)Cl]^+ \xrightarrow[-H_2O]{+DCC} Pt/PtO/[Si(CH_2)_3NH(CH_2)_2NHCO\text{-}4\text{-}pyRuCl(bpy)_2]^+$$

Procedure 2 (py-Silane Surface)

$$Pt/PtO + Cl_3SiCH_2CH_2\text{-}4\text{-}py \rightarrow Pt/PtO/SiCH_2CH_2\text{-}4\text{-}py$$

$$Pt/PtO/SiCH_2CH_2\text{-}4\text{-}py + \text{“}[Ru(bpy)_2(DME)Cl]^{+}\text{”} \xrightarrow[-DME]{} Pt/PtO/[SiCH_2CH_2\text{-}4\text{-}pyRuCl(bpy)_2]^+$$

DME is 1,2-dimethoxyethane

The second attachment scheme is based on the displacement of a weakly bound ligand in the inner coordination sphere of a ruthenium complex by a pyridyl ligand which had been preattached to the electrode surface: in this case, the py-silane surface, Pt/PtO/$SiCH_2CH_2$-4-py. The experiments were carried out by allowing the dimethoxyethane (DME) solution

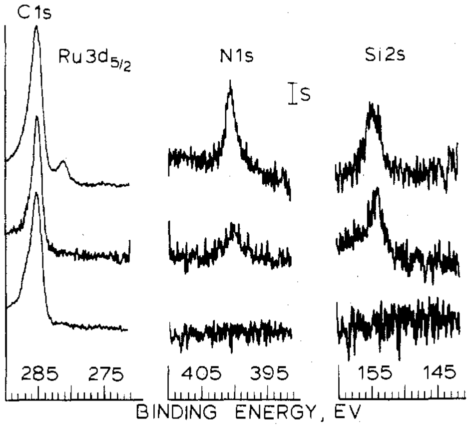

Figure 1. X-ray photoelectron spectra of chemically modified Pt/PtO electrodes: (A) Pt/PtO/en/$[Ru(bpy)_2(bpy\text{-}diacid)]^{2+}$ electrode; (B) Pt/PtO/en electrode; (C) control. The Pt/PtO was treated with an CH_3CN solution containing $[Ru(bpy)_2(bpy\text{-}diacid)]^{2+}$ for 20 h. S = 1450 counts for C 1s and Ru $3d_{5/2}$, 390 counts for N 1s, and 220 counts for Si 2s.

which contained both the chelate $[(bpy)_2Ru(DME)]^{2+}$ and $[(bpy)_2Ru(DME)Cl]^+$ to react with the silanized electrode. The DME solutions containing the solvent-bound complexes were generated by adding less than a 2:1 amount of $AgPF_6$ to $Ru(bpy)_2Cl_2$ dissolved in DME and filtering off the AgCl which formed. The choice of the DME complex was based on earlier work where it was shown that the bound DME group could be displaced in subsequent reactions by ligands like pyridine.[9] The Ru complex or complexes in DME are designated here as complex IV.

Attachment and Surface Structure. The attachment chemistry for the four different ruthenium complexes was examined by a combination of XPS and cyclic voltammetry experiments. A series of control experiments was carried out in order to distinguish adsorption of the complexes on the electrode surface from attachment by the desired forms of covalent bonding.

Figure 1A shows the XPS of a Pt/PtO/en electrode surface on which all steps for the attachment of III, $[Ru(bpy)_2(bpy\text{-}diacid)]^{2+}$, had been carried out. An XPS band for Ru $3d_{5/2}$ is clearly visible at the base of the ubiquitous C 1s peak. The binding energy, 280.8 eV, for the band is in good agreement with that obtained for the salt $[Ru(bpy)_2(bpy\text{-}diacid)][PF_6]_2$ (280.9 eV). The N 1s band is enhanced over that observed on a Pt/PtO/en surface (Figure 1B), consistent with the added nitrogen atoms of the bound bpy ligands. A cyclic voltammogram of a Pt/PtO/en electrode which had been reacted with the bpy-diacid complex in the presence of DCC is illustrated in Figure 2A. A wave for the surface-bound complex is observed at a formal potential of $E^{0\prime} = +1.33$ V vs. SSCE. This value is very near that (+1.36 V) found for the unattached complex in acetonitrile. The surface wave exhibits the symmetry, small peak potential separation (ΔE_p), and peak current–potential scan rate proportionality anticipated from theory for a surface-localized charge-transfer state.[11] The surface wave is broader than predicted for the ideal case of no interaction with the surface or between surface-attached neighbors.[12] For the noninteracting case, the full width at half-maximum for the cyclic voltammetric wave, E_{FWHM}, should be 90.6 mV. The area of the surface wave decreases slightly during the first few cyclical potential scans but then remains essentially constant, changing only slowly over thousands of potential scans. The scans were carried out at a sweep rate of 200 mV/s. The surface wave for the particular electrode shown in Figure 2A remained observable for about 4000 scans. Among numerous samples of the four different immobilized ruthenium complexes, the stability of the surface waves varied widely, with lifetimes (the number of scans until the surface wave no longer was observable) ranging from as few as 2000 to as many as 70 000 continuously repeated scan cycles. A more detailed analysis of the surface wave decay and the observed broadening is presented below.

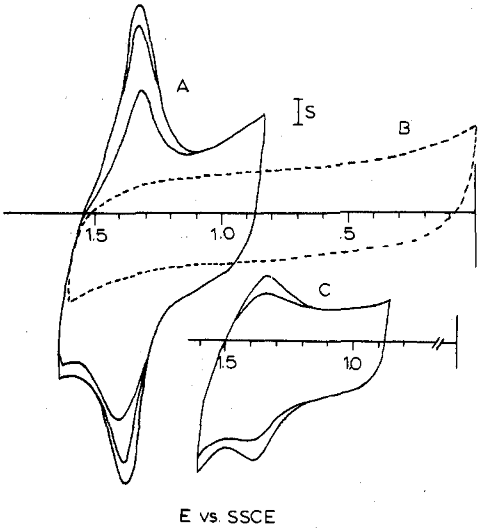

Figure 2. Cyclic voltammograms for the Pt/PtO/en/$[Ru(bpy)_2(bpy\text{-}diacid)]^{2+}$ electrode in $[Et_4N^+][ClO_4^-]/CH_3CN$ at 200 mV/s: (A) Pt/PtO/en/$[Ru(bpy)_2(bpy\text{-}diacid)]^{2+}$ electrode after 15, 71, and 520 scans (S = 1.9 $\mu A/cm^2$); (B) the Pt/PtO was treated with an CH_3CN solution of the bpy-diacid complex for 22 h (S = 3.8 $\mu A/cm^2$); (C) the Pt/PtO was treated with an CH_3CN solution of the bpy-diacid complex plus DCC for 20 h, and the curves were obtained after 14 and 38 scans (S = 1.9 $\mu A/cm^2$).

A series of control experiments was carried out based on the systematic omission of reaction components involved in preparing the chemically modified surfaces. In the amide-coupling scheme used for complexes I–III, control experiments were carried out omitting both en-silane and DCC, en-silane only, or DCC only, with the other steps in the overall coupling scheme remaining the same. When both en-silane and DCC were omitted, that is, when Pt/PtO electrodes were contacted with solutions of I, II, or III, there was neither XPS (Ru $3d_{5/2}$, N 1s peaks above background) nor electrochemical evidence for bound complex, as illustrated for the bpy-diacid complex (III) in Figures 1C and 2B. The evidence suggests that these complexes do not chemisorb or chemisorb so weakly that when bound, they do not survive the rinsing procedures used.

Reaction of the Pt/PtO electrode with III in the presence of DCC (omitting en-silane) gives a relatively small Ru $3d_{5/2}$ band and a small (ca. 15% of Figure 2A) unstable electrochemical wave as illustrated in Figure 2C. The DCC-induced surface complex is weakly bound. In fact, the small initial decay of the wave for the Pt/PtO/en/bpy-diacid surface shown in Figure 2A probably has as its origin this weakly bound complex. It disappears within 10–100 potential scans (Figure 2A), leaving a much more stable species which we believe to be the en-silane covalently attached complex.

A third control reaction, in which DCC was omitted from the reaction of Pt/PtO/en with III, leads to XPS and electrochemical responses identical in all respects (including stability) with those in experiments where DCC was added, except that the XPS and electrochemical responses were 3–10 times smaller. The result points out that DCC facilitates but is not essential for surface amide bond formation and is similar to results obtained earlier in other surface amidization studies.[13]

For the DME complex (IV), the control studies involved exposing electrode surfaces to solutions where either all of the reaction components were present or all were present except for the py-silane reagent. With all components added, XPS show prominent Ru $3d_{5/2}$, N 1s, and Si 2s bands much as shown in Figure 1A, and well-defined cyclic voltammograms are obtained which resemble those of Figure 2A, at least qualitatively. In the control experiment where the py-silane was omitted, there was no evidence for a surface-bound complex. Once again, if simple adsorption does occur, the adsorbed complex is sufficiently weakly bound that it does not survive the rinsing process.

Potentials for (2,2′-bpy)$_2$Ru$^{\text{III/II}}$ couples vary systematically with changes in the remaining two ligands.[4] This is an observation of some value here since it suggests that the formal potential for the surface-bound complexes can be used to infer the chemical nature of the attached groups. Table II compares $E^{0\prime}_{\text{surf}}$ with formal potentials, $E^{0\prime}_{\text{soln}}$, for the Ru$^{\text{III/II}}$ couples of closely related complexes in solution. It is clear from the data that differences between surface-bound and homogeneous formal potentials are quite small, which supports our contentions that the complexes are amide bound to the Pt/PtO/en surface and that the inner coordination spheres of the complexes are undisturbed by the attachment chemistry. For the surface complex prepared by the reaction between the py-silanized surface and the DME complex, the $E^{0\prime}_{\text{surf}}$ result is consistent with the bound species being the chloro–pyridyl complex $[\sim\text{pyRuCl(bpy)}_2]^+$, and, as expected, the potential value is very close to that for the amide-attached complex $[\sim\text{NHCOpyRuCl(bpy)}_2]^+$, prepared by the reaction between the en-silane surface and $[\text{Ru(bpy)}_2(4\text{-pyCO}_2\text{H})\text{Cl}]^+$.

Properties of Pt/PtO/en/III Electrodes. The bpy-diacid complex (III) is of special interest to us since it is a close chemical relative of the well-known $[\text{Ru(bpy)}_3]^{2+}$ complex.[14] A cyclic voltammogram of the attached complex is shown in Figure 2A, and additional electrochemical data are presented in Table II. Earlier attempts in our laboratory to attach III to en-silanized SnO$_2$, RuO$_2$, and Pt/PtO electrodes were unsuccessful. This may be, in part, because the coupling reaction has proven to be quite sensitive to the state of purification of the en-silane reagent used in the silanization step. As obtained commercially, the en-silane can be quite impure. If the reagent is doubly vacuum distilled initially and redistilled just prior to use, it is possible to obtain, with consistency, the range of coverages indicated for the Pt/PtO/en/III surfaces in Table II. Surface coverages were determined by calculating the total charge passed in an oxidative or reductive sweep based on measurements of the area under the voltammetric wave. On the basis of molecular models, it can be estimated that a monomolecular coverage of the complex on the surface would give a surface coverage value of ca. 8×10^{-11} mol/cm^2, using an average molecular radius of 7.1 Å. Coverage values for surfaces containing attached III are consistently near this value (Table II).

$E^{0\prime}_{\text{surf}}$ values for the attached bpy-diacid complex are consistently 20–30 mV more negative than the solution value for the couple $[\text{Ru(bpy)}_2(2,2'\text{-bpy-4,4}'\text{-diacid})]^{3+/2+}$. The magnitude and direction of the shift are consistent with the change in substituent effect between the complex in solution, where the bpy substituents are acid groups, and the surface complex, where the substituents are amide groups. We have no convincing evidence, however, as to whether the surface bonding occurs via one or both of the carboxylic acid groups. Figure 2A gives no indication of a double wave which might be expected if there were both singly and doubly amide-bound complexes on the surface. However, given the small differences in potential expected for the two forms, two separate waves would probably be unresolvable by cyclic voltammetry. The cathodic surface waves observed for the bound and solution forms of III (Table II), which involve reduction at the bpy ligands, are also in close agreement.

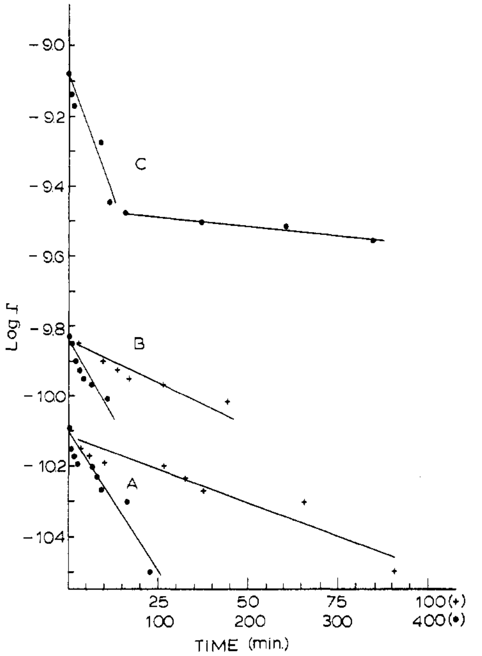

Figure 3. First-order decay plots for chemically modified Pt/PtO electrodes. The time axis refers to the time spent as Ru$^{\text{III}}$ and the data are shown plotted on two different time scales to facilitate comparisons. (A) Pt/PtO/en/$[\text{Ru(bpy)}_2(\text{bpy-diacid})]^{2+}$, $k = 8.6 \times 10^{-3}$ s^{-1}, correlation coefficient = 0.95; (B) Pt/PtO/en/$[\text{Ru(bpy)}_2(4\text{-pyCO}_2\text{H})\text{Cl}]^+$, $k = 1.2 \times 10^{-2}$ s^{-1}, correlation coefficient = 0.96; (C) Pt/PtO/py$[\sim\text{Ru(bpy)}_2\text{Cl}]^+$, for initial rapid decay $k = 1.4 \times 10^{-2}$ s^{-1}, correlation coefficient = 0.96, for slower decay $k = 6.1 \times 10^{-4}$ s^{-1}, correlation coefficient = 0.98.

As noted above, the Ru$^{\text{III/II}}$ cyclic voltammetric wave of the bound bpy-diacid complex gradually decays upon repetitive potential scanning. No other waves appear during the decay, and XPS experiments show that ruthenium is lost from the electrode surface. Figure 3A presents a first-order plot of the coverage of III during the decay process. Following the initial rapid decay, the electrode degradation process follows approximately first-order kinetics. A rate constant for surface-state decay of 8.6×10^{-3} s^{-1} (correlation coefficient = 0.95) can be calculated from the slope of the plot in Figure 3A ($k = 2.303$ (slope)). The decay process clearly is initiated by the electrochemical oxidation of Ru(II) to Ru(III) since the electrodes in the Ru(II) state are otherwise very stable to storage in acetonitrile and other solvents. It seems unlikely that the decay is associated with the electron-transfer processes to and from the electrode. If that were the case, the rate of decay would be proportional to the total number of scans and the integrated time dependence would almost certainly not be logarithmic. Given the stability of the surfaces in the Ru(II) state, and the logarithmic time dependence, it seems reasonable that the instability of the surface arises in the Ru(III) state. As a consequence, the time axis in Figure 3 refers to the time spent in the Ru(III) state. The estimated times in the Ru(III) state were calculated by taking twice the time needed to vary the potential at the electrode from 100 mV negative of $E^{0\prime}$ for the Ru$^{\text{III/II}}$ couple to the anodic limit of an individual scan multiplied by the total number of scans. Although this procedure was clearly somewhat arbitrary, it should be noted that for the $[\sim\text{pyRuCl(bpy)}_2]^+$ electrode described later, it gave essentially the same results as a procedure where the ruthenium site was held as Ru(III) and periodic scans were taken to establish the extent of decay from the surface.

Although we do not have detailed information about the nature of the decay process, it is probably associated with the known ability of ruthenium(III)–bipyridyl complexes to act as facile oxidants of a variety of organic substrates. Another possibility is that it is associated with the presence of trace amounts of water which can be oxidized by $[\text{Ru(bpy)}_3]^{3+}$, but

Table I

electrode surface	starting complex	reacn solvent	reacn time, h	rinsing procedure[a]
Pt/PtO/en	I	CH_3CN + DCC[b]	26	CH_3CN (2×), acetone (2×), CH_2Cl_2 (2×)
Pt/PtO/en	II	CH_2Cl_2 + DCC	26[c]	acetone (3×), CH_2Cl_2 (3×)
Pt/PtO/en	III	CH_3CN + DCC	24	CH_3CN (2×), acetone (2×), CH_2Cl_2 (2×)
Pt/PtO/py	$[Ru(bpy)_2(DME)]^{2+}$ (IV)[d]	DME	24[e]	DME (2×), CH_3CN (2×), CH_2Cl_2 (2×)

[a] Total rinsing time averages 20 h. [b] DCC is *N,N′*-dicyclohexylcarbodiimide. [c] Reaction run in the dark. [d] A solution produced by the reaction between $Ru(bpy)_2Cl_2$ and $AgPF_6$ in dimethoxyethane. Note the comments on this couple in the text. [e] Thoroughly degassed to avoid μ-oxo-bridged dimer formation.[8]

Table II. Electrochemical Results

proposed surface complex	$E^{0\prime}_{surf}$,[a] V vs. SSCE	ΔE_p, mV	E_{FWHM}, mV	$10^{10}\Gamma_{corr}$,[b] mol/cm²	soln analogue	$E^{0\prime}_{soln}$, V vs. SSCE
$Pt/PtO/[Si(CH_2)_3NH(CH_2)_2NHCO\text{-}pyRu(bpy)_2(pyCOOH)]^{2+}$ [c] (I)	1.31	43	125	0.60	$[Ru(bpy)_2(py\text{-}CONH_2)_2]^{2+}$	1.32_5
	1.32	55	120	0.68	$[Ru(bpy)_2(py\text{-}COOH)_2]^{2+}$	1.35_6
	1.31	40	120	0.75		
	1.31	52	120	1.2		
	1.30	55	125	1.5		
	1.30	40	130	2.0		
	1.29	40	130	3.0		
	1.31[d]					
$Pt/PtO/[Si(CH_2)_3NH(CH_2)_2NHCO\text{-}pyRu(bpy)_2Cl]^+$ (II)	0.80	45	135	0.60	$[Ru(bpy)_2(py\text{-}COOH)Cl]^+$	0.81_6
	0.79	55	130	0.68	$[Ru(bpy)_2(py)Cl]^+$	0.80
	0.77	45	175	0.88		
	0.79	30	120	1.1		
	0.79	30	140	1.1		
	0.79[d]					
$Pt/PtO/\{Si(CH_2)_3NH(CH_2)_2NHCO(bpy\text{-}diacid)Ru(bpy)_2\}^{2+}$ [c] (III)	1.34	30	150	0.21	$[Ru(bpy)_2(bpy\text{-}diacid)]^{2+}$	1.36
	1.33	20	140	0.31		−1.38[e]
	1.33	30	160	0.53		−1.58[e]
	1.31	100	160	0.65		
	1.34	25	130	0.78		
	1.32	25	150	0.79		
	1.34	80	180	0.89		
	1.32	60	150	0.97		
	1.33	90	160	1.4		
	−1.36 ± 0.02[e]					
	−1.52 ± 0.02[e]					
$Pt/PtO/[Si(CH_2)_2\text{-}pyRu(bpy)_2Cl]^+$ (IV)	0.76	30	160	0.94	$[Ru(bpy)_2(py)Cl]^+$	0.80
	0.76	20	120	1.3		−1.50[e]
	0.77	45	185	1.5		−1.76[e]
	0.76	18	170	1.6		
	0.75	60	230	1.9		
	0.77	40	(200)[f]	3.5		
	0.75	30	155	3.7		
	0.75	45	(160)[f]	4.3		
	0.77	50	(180)[f]	4.8		
	0.77	85	(190)[f]	4.8		
	−1.48 ± 0.02[e]					
	−1.69 ± 0.02[e]					

[a] Average of oxidation and reduction peak potentials. [b] Corrected for 1.3 surface roughness factor. [c] Unknown whether second amide bond forms or not. [d] Very low Γ, $E^{0\prime}$ determined by phase-selective AC voltammetry. [e] Reduction waves. All other potentials are for $Ru^{3+/2+}$. [f] Wave is asymmetrical.

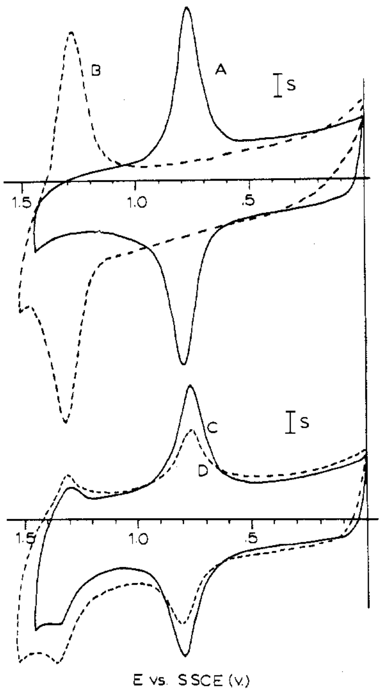

Figure 4. Cyclic voltammograms for Pt/PtO/en/$[Ru(bpy)_2(4\text{-}pyCO_2H)Cl]^+$ and Pt/PtO/en/$[Ru(bpy)_2(4\text{-}pyCO_2H)_2]^{2+}$ electrodes in 0.1 M $[Et_4N^+][ClO_4^-]/CH_3CN$ at 200 mV/s: (A) Pt/PtO/en/$[Ru(bpy)_2(4\text{-}pyCO_2H)Cl]^+$ electrode (S = 3.7 $\mu A/cm^2$); (B) Pt/PtO/en/$[Ru(bpy)_2(4\text{-}pyCO_2H)_2]^{2+}$ electrode (S = 3.8 $\mu A/cm^2$); (C and D) Pt/PtO/en/$[Ru(bpy)_2(4\text{-}pyCO_2H)Cl]^+$ electrode from A after 590 and 1500 scans, showing the substitution of CH_3CN for coordinated chloride (S = 3.7 $\mu A/cm^2$).

with decomposition of the complex.[19]

Properties of Pt/PtO/en/I and Pt/PtO/en/II Electrodes. Cyclic voltammograms for the chemically bonded mono- and bis(isonicotinic acid) complexes I and II are shown in parts A and B of Figure 4, and additional data are given in Table II. The surface waves are symmetrical with small ΔE_p values and with $E^{0\prime}_{surf}$ values which agree quite well with those of the related complexes in solution. Surface coverages are consistent with monolayer coverage levels, except for a few examples of immobilized I where Γ is 2–3 times larger. The multilayer coverage apparently arises because of polymerization of the en-silane reagent on the surface. Except for enhanced coverages, however, the latter samples exhibit no distinctive behavior.

If a solution containing a mixture of the mono- and bis(isonicotinic acid) complexes is allowed to react with a Pt/PtO/en surface, the resulting electrode exhibits separate surface waves for both complexes at their expected $E^{0\prime}_{surf}$ values. The relative coverages, as determined by the amount of charge transfer (calculated by the areas under the voltammetric waves), are within a factor of 2 of that of the relative concentrations of the two complexes in the reaction solution. The experiment suggests that the reactivities of the two complexes in the surface-coupling process are similar and raises the possibility of preparing surfaces which bear a graded series of redox couples having different redox potentials.

The surface waves for attached I and II are quite persistent, with lifetimes in excess of 10 000 potential scan cycles for II. Of the two surfaces I and II, the chloro–pyridyl surface (II) has more exploitable points and was investigated in further detail. A special feature associated with II is the possibility of having ligand-substitution reactions take place while the complex is bound to the surface. Solution spectral and electrochemical studies[15] show that in acetonitrile $[(bpy)_2Ru(py)Cl]^+$ undergoes a photochemical substitution reaction in which coordinated pyridine is replaced by CH_3CN to give $[(bpy)_2Ru(CH_3CN)Cl]^+$ (λ_{max} 480 nm; $E^{0\prime}$(Ru(III),Ru(II)) = 0.86 V).[4] The complex is stable in acetonitrile for days in the dark. On the surface, however, the chloro–pyridyl complex shows a rather dramatic change in reactivity. With a 75-W light bulb held close to the surface, extended photolysis (3 days) of attached II in CH_3CN or CH_2Cl_2 produced no loss of the surface-bound complex. A probable explanation for the quenching of the photochemical behavior is that the attached complex is in close proximity to the metal electrode; electrode surfaces are well-known as efficient quenchers of molecular excited states. Our observations are of value for two reasons. They suggest that reagents which are photochemically labile in solution can be stabilized in the chemically attached state, and, if the quenching mechanism is by electron transfer, they could lead to useful photovoltaic effects.

Another difference in chemical reactivity which was unexpected, given the results of related solution studies, is that, following a series of potential scans through the Ru(II) → Ru(III) region, a new wave appeared at +1.32 V at the expense of the initial wave at 0.79 V for the $[\sim NHCO\text{-}pyRuCl(bpy)_2]^{2+/+}$ attached couple (Figure 4A,C,D). Under the same conditions, the electrodes are stable in the Ru(II) form. The $E^{0\prime}_{surf}$ value for the new surface wave is consistent with having the acetonitrile complex $[NHCO\text{-}pyRu(CH_3CN)(bpy)_2]^{2+}$ on the surface. In acetonitrile solution, the Ru^{III} complex $[(bpy)_2Ru(py)Cl]^{2+}$ is far less photoactive than is $[(bpy)_2Ru(py)Cl]^+$ and is stable indefinitely toward thermal substitution. The rate of substitution of acetonitrile for the chloro group is not noticeably affected by whether or not the surface is exposed to light.

We do not yet understand the origin of the lability of the chemically attached chloro group. It may involve an assisted substitution process at Ru^{III} in the surface matrix, or it may be an accompanying feature of the electron-transfer act to and from the electrode. In the latter case, the result would suggest that electron transfer to and from the bound complex involves, at least in part, an "inner-sphere" mechanism where the chloro group acts as a bridge between the chemically attached Ru and a redox site on the metal surface.

In a repetitive cycling experiment, the decay of the surface wave for the attached chloro–pyridine complex (II) appears to follow first-order kinetics as did the decay process for chemically attached complex III. The decay data in Figure 3B follow first-order kinetics, and a first-order kinetic plot gave an apparent constant of $1.2 \times 10^{-2}\ s^{-1}$ (correlation coefficient = 0.96). The decay in the chloro–pyridine complex surface wave at +0.79 V is paralleled by a growth in the wave at 1.32 V for the attached acetonitrile–pyridine complex. However, the amount of acetonitrile–pyridine complex formed is distinctly less than the initial amount of chloro–pyridine complex, as shown by comparisons in relative peak heights. This result shows that degradation and loss of Ru from the surface must be occurring simultaneously with the induced substitution of acetonitrile for the bound chloro group.

Properties of the Pt/PtO/py/IV Electrodes. The electrodes prepared by using the py-silane reagent in the initial silanization step represent a second mode of attaching 2,2′-bipyridyl complexes of ruthenium to electrode surfaces. The displacement of weakly bound solvent ligands in net substitution reactions has provided a useful synthetic route to a series of bipyridyl complexes,[16] and the use of the attached py-silane group as a ligand was an attempt to transpose the known solution chemistry to syntheses on electrode surfaces. Dimethoxyethane proved to be a better reaction medium than acetone even though acetone has been used extensively in the solution synthetic chemistry.[9,16] As noted above, from the

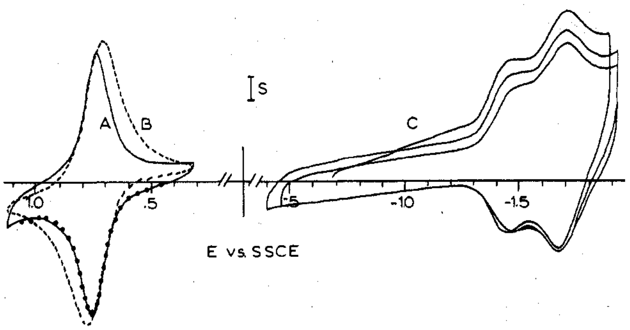

Figure 5. Cyclic voltammograms for Pt/PtO/py{∼Ru(bpy)$_2$Cl]$^+$ (IV) electrodes in 0.1 M [Et$_4$N$^+$][ClO$_4^-$]/CH$_3$CN at 200 mV/s: (A) comparison of experimental (—) and theoretical (●) cyclic voltammograms where there is ca. monolayer coverage (S = 5.7 μA/cm^2); (B) Pt/PtO/py/IV electrode with multilayer coverage (S = 37.4 μA/cm^2); (C) Pt/PtO/py/IV electrode when scanned cathodically on the fourth, fifth, and sixth scans (S = 12.2 μA/cm^2).

results of a series of experimental blanks, there is no evidence that surface adsorption occurs to any significant degree on the unsilanized surfaces.

A cyclic voltammogram of a Pt/PtO/py/IV electrode is illustrated in Figure 5A with additional data given in Table II. The small peak-to-peak potential separation, the symmetry of the peaks, and the excellent definition of the wave above background are all quite similar to those for electrodes to which the amide-bound chloro–pyridine complex is attached (Figure 4A). Given the nature of the attachment chemistry and the probable existence of both chelated and unidentate dimethoxyethane complexes in the reaction solution used, we initially assumed that we might possibly find evidence for as many as three different surface-attached complexes, [Ru(bpy)$_2$(py∼)$_2$]$^{2+}$, [Ru(bpy)$_2$(py∼)Cl]$^+$, and [Ru(bpy)$_2$(DME)(py∼)]$^{2+}$. However, the only surface wave we can find is that for the chloro–pyridine complex. We have obtained XPS evidence for bound chloride on these electrodes. The origin of the chloride group may be from the less than stoichiometric amount of AgPF$_6$ added to the Ru(bpy)$_2$Cl$_2$–DME reactant solution or from residual chloride ion (originating from the silane) adsorbed on the surface during the silanization step.

As commercially obtained, the py-silane reagent, which is highly reactive, is typically partially polymerized. The silanization reactions were conducted by extracting the solid reagent with dry toluene and treating the Pt/PtO surface with the extract. The extracts apparently contain both monomeric silane plus soluble, short-chain polymeric components where the polymer backbone is based on –Si–O–Si– links. With reasonable frequency, the procedure described above leads to surfaces bearing coordinated ruthenium at coverages too large to be compatible with monomolecular layers. Taking monolayer coverage as ca. 9 × 10^{-11} mol/cm^2,[17] the data in Table II show that coverages of up to 5–6 monolayer equiv of the complex were obtained. The data in Table II show that $E^{0\prime}_{\text{surf}}$ does not vary significantly with coverage, but ΔE_{p} tends to increase on the multilayer electrodes. The multilayer electrodes also develop a tailing asymmetry for both the anodic and cathodic peaks as illustrated in Figure 5B. One explanation for the tailing is slow charge transfer or transport from a portion of the immobilized complexes. Superimposing their cyclic voltammetric response (with large ΔE_{p} values) on the one for those complexes undergoing rapid charge transfer/transport (with $\Delta E_{\text{p}} \approx 0$) would give rise to the overall peak tailing. If this interpretation is correct, the reasons for slow charge transfer/transport for the multilayer surfaces are of interest and are under study. Significant factors could be the existence of redox sites at spatially remote locations from the surface, reduced motional freedom due to electrostatic effects, cross-linking of the siloxane polymer, or slow counterion transport which is a process necessary to maintain charge balance during the electron-transfer reactions.

The stability of the Pt/PtO/py/IV electrodes is greater than that for the other electrodes. Typically, the electrodes can be continuously cycled through 15 000 oxidation/reduction cycles of the Ru$^{\text{III/II}}$ couple at a scan rate of 200 mV/s. A number of the multilayer samples exhibited surface waves that persisted for over 70 000 cycles. Electrodes of both the monolayer and multilayer variety have been stored in the presence of air and light for over 1 year with little change as shown by their cyclic voltammetric properties. The decay of the Ru$^{\text{III/II}}$ wave at +0.77 V was accompanied, as for the Pt/PtO/en/II electrodes, by growth of a wave at +1.32 V that we ascribe to the attached acetonitrile complex {∼pyRu(CH$_3$CN)(bpy)$_2$]$^{2+}$. A first-order decay plot for a multilayer electrode is shown in Figure 3C, where again the time axis is taken as time spent as Ru(III). An initial period of relatively rapid decay was observed, for which k = 1.4 × 10^{-2} s^{-1} (correlation coefficient = 0.96) which is similar in magnitude to values obtained for the decay of the Pt/PtO/en/II and Pt/PtO/en/III surfaces. Following the initial step, a much slower decay process occurs for which k = 6.1 × 10^{-4} s^{-1} (correlation coefficient = 0.98) was estimated. The results of the kinetic analysis of the Pt/PtO/en/IV electrodes suggest that there may be a mixed surface population composed of one type of site (monomers?) having decay properties which are similar to those of the attached complexes II and III where there are monolayer coverages and of a new, much more stable site within the polymer matrix. If this interpretation is correct, from the surface coverage data and the relative amounts of short- and long-lived sites, the attached polymeric sites would have an effective chain length much greater than the value of 5–6 determined electrochemically since that value represents an average over both monomers and polymers.

Ligand-Based Reductions. In their solution electrochemistry, ruthenium–polypyridyl complexes are known to undergo reversible reductions localized on the bpy ligands,[4] and such reactions have also been found for the attached complexes in this work. Figure 5C illustrates the cathodic surface waves observable on a Pt/PtO/py/IV electrode, and Table II compares the $E^{0\prime}_{\text{surf}}$ values for these waves with data for the solution analogue. The charge under each cathodic wave is within 10% of that found for the corresponding Ru$^{\text{III/II}}$ wave, which is satisfactory agreement, given the much poorer definition of the cathodic waves. From comparisons of total charge passed, obtained by measuring areas under the waves, each reductive process can be assumed to be a one-electron process which is also the case for [Ru(bpy)$_2$(py)Cl]$^+$ in solution.

The electrodes proved to be quite unstable toward cycling through the cathodic waves. An average lifetime of about 20 cycles was typical at a scan rate of 200 mV/s. The decay of the cathodic surface waves was accompanied by loss of the Ru$^{\text{III/II}}$ wave at +0.77 V. The same type of instability has also been observed toward reductive cycling for the Si/SiO/en-[Ru(bpy)$_2$(bpy-diacid)]$^{2+}$ surface. The origin of the instability is not clear, especially given the long-term stability of [Ru(bpy)$_3$]$^+$ in dry, deaerated acetonitrile.[20]

Shape of the Current–Potential Waves for the Attached Complexes. Except for the case of complex IV where a multilayer surface was obtained, all surface cyclic voltammetric waves observed in this study were symmetrical. If surface concentration and activity are equated in the theory for the current–potential relationship, a peak width at half-maximum of 90.6 mV is predicted.[12c] All complexes exhibit waves broader than this as seen in Table II by the E_{FWHM} data. Brown and Anson[12d] have discussed cyclic voltammetric surface waves for strongly adsorbed quinones on carbon in

Table III. Surface Interaction Parameters

attached complex	potl scan	$10^{10}\Gamma$,[a] mol/cm^2	$10^{-9}r$	scan rate, mV/s	E_{FWHM},[b] mV
IV	anodic	1.66	−4.84	200	134
	anodic	5.03	−1.19	200	123
III	cathodic	1.49	−4.63	200	128
	anodic	1.36	−4.55	200	
II	cathodic	1.54	−3.39	100	
	anodic	1.51	−3.82	100	122
	anodic	1.21	−7.56	100	140
	anodic	1.10	−8.39	200	142
	anodic	0.98	−9.84	100	144
	anodic	0.93	−11.0	200	146

[a] To correct for electrode roughness, divide by 1.3. [b] Values resulting from computer comparison of theory with the experimental wave agree with manually obtained parameters, in general, but are more precise since computation uses a more sophisticated base-line approximation.

terms of a surface activity which is exponentially related to surface concentration and surface nonideality or interaction parameters for the oxidized and reduced species, r_{Ox} and r_{Red}, respectively. From their treatment, negative values of the nonideality parameters indicate repulsive or destabilizing interactions and correspond to broadened waves. In earlier work we have shown that the shape of the current–potential waves predicted by this theory does fit the electrochemical behavior of molecules attached to electrode surfaces by organosilane reagents.[13,18] However, certain details of the theory do not satisfactorily represent experimental observations. The theory predicts that if $r_{\mathrm{Red}} = r_{\mathrm{Ox}}$, the formal potential of the surface-attached redox site should not depend on its surface coverage, Γ. Since from Table II we see no systematic variation of $E^{0\prime}_{\mathrm{surf}}$ with Γ, we have equated $r_{\mathrm{Ox}} = r_{\mathrm{Red}} = r$ in the present comparison.

Using a computational approach described elsewhere,[18] we compared surface waves for the complexes attached in this study to those from the Brown and Anson[12d] surface activity theory. An illustrative comparison is shown for Figure 5A, where theoretical points are superimposed on the experimental response, and computed results are given in Table III. In general, the correspondence of theory and experimental current–potential responses, in terms of wave shape, is quite good. In all cases, negative values of the interaction parameter were obtained. Also, values for $E^{0\prime}_{\mathrm{surf}}$, E_{FWHM}, and Γ from the computation agree well with those obtained from raw data when estimated base lines are used.

Several observations can be made on the derived values of r in Table III. First, we have previously[18] observed for an immobilized ferrocene group that the interaction parameter seemed to vary according to whether data had been taken on a positive- or negative-going potential scan. No such dependency has been found for the ruthenium complexes as shown by data for complexes II and III for consecutive anodic and cathodic potential scans for given electrodes. Secondly, data for complex II taken over a range of surface coverages yield an approximately inverse relationship between interaction parameter and coverage. This dependency, seen also for an immobilized ferrocene,[13] is not anticipated by the theory, and we have no suitable interpretation at present. Lastly, if one compares the surface activity theory to results obtained for a multilayer surface, derived from complex IV, mismatch occurs in the tail of the current–potential peak, but the fit on the leading edge is rather good. This comparison can be regarded as an estimate of the interaction problem for the fast charge transfer component on the multilayer electrodes. The data of Table III show that its interaction parameter is somewhat smaller than that observed on the monolayer electrodes.

Conclusions

The work described here demonstrates that polypyridyl complexes of ruthenium can be covalently attached to silanized platinum oxide surfaces by two different synthetic approaches. Once attached, the complexes appear to retain the chemical properties of their homogeneous solution analogues to a large degree, as shown by similarities in redox potentials and chemical reactivity. However, an efficient photochemical process in solution is quenched apparently due to the proximity of the immobilized complex to the metal electrode.

Due to their relatively high stability to cycling between oxidation states, our ability to manipulate the chemical nature and reactivity of the attached complex by judicious variation in the coordinated ligands, and the known properties of related complexes as redox catalysts in solution, these chemically modified surfaces are attractive as possible precursors to chemically tailored catalytic electrodes.

Acknowledgment. This research was supported in part by grants to T.J.M. and R.W.M. from the National Science Foundation. The authors gratefully acknowledge the help of Dr. J. L. Walsh and Dr. B. P. Sullivan in carrying out some of the synthetic work.

Registry No. I, 71171-45-4; II, 71171-47-6; III, 64189-98-6; IV, 69063-73-6; *cis*-Ru(bpy)$_2$Cl$_2$, 19542-80-4; en-silane, 1760-24-3; py-silane, 17082-70-1.

References and Notes

(1) (a) P. R. Moses and R. W. Murray, *J. Am. Chem. Soc.*, **98**, 7435 (1976); (b) P. R. Moses, L. M. Wier, J. C. Lennox, H. O. Finklea, J. R. Lenhard, and R. W. Murray, *Anal. Chem.*, **50**, 576 (1978); (e) J. R. Lenhard, R. Rocklin, H. Abruña, K. Willman, K. Kuo, R. Nowak, and R. W. Murray, *J. Am. Chem. Soc.*, **100**, 5213 (1978); K. Itaya and A. J. Bard, *Anal. Chem.*, **50**, 1487 (1978); (e) C. A. Koval and F. C. Anson, *ibid.*, **50**, 223 (1978); (f) M. Fujihira, T. Osa, D. Hursh, and T. Kuwana, *J. Electroanal. Chem.*, **88**, 285 (1978).

(2) (a) P. R. Moses, L. Wier, and R. W. Murray, *Anal. Chem.*, **47**, 1882 (1975); (b) P. R. Moses and R. W. Murray, *J. Am. Chem. Soc.*, **98**, 7435 (1976); (c) *J. Electroanal. Chem.*, **77**, 393 (1977); (d) M. S. Wrighton, R. G. Austin, A. B. Bocarsly, J. M. Bolts, O. Haas, K. D. Legg, L. Nadjo, and M. Palazzotto, *ibid.*, **87**, 429 (1978); (e) M. S. Wrighton, R. G. Austin, A. B. Bocarsly, J. M. Bolts, O. Haas, K. D. Legg, L. Nadjo, and M. C. Palazzotto, *J. Am. Chem. Soc.*, **100**, 1602 (1978); (f) M. S. Wrighton, M. C. Palazzotto, A. B. Bocarsly, J. M. Bolts, A. B. Fischer, and L. Nadjo, *ibid.*, **100**, 7264 (1978).

(3) J. R. Lenhard and R. W. Murray, *J. Electroanal. Chem.*, **78**, 195 (1977).

(4) D. J. Salmon, Ph.D. Thesis, The University of North Carolina, Chapel Hill, 1977.

(5) V. Balzani, F. Bolletta, M. T. Gandolfi, and M. Maestri, *Top. Curr. Chem.*, **75**, 1 (1978); T. J. Meyer, *Acc. Chem. Res.*, **11**, 94 (1978).

(6) F. R. Keene, D. J. Salmon, and T. J. Meyer, *J. Am. Chem. Soc.*, **99**, 4821 (1977); B. A. Moyer, M. Thompson, and T. J. Meyer, submitted for publication.

(7) H. Angerstein-Kozlowska, B. E. Conway, and W. B. A. Sharp Jr., *J. Electroanal. Chem.*, **43**, 9 (1973).

(8) T. R. Weaver, T. J. Meyer, S. A. Adeyemi, G. M. Brown, R. P. Eckberg, W. E. Hatfield, E. C. Johnson, R. W. Murray, and D. Untereker, *J. Am. Chem. Soc.*, **97**, 3039 (1975).

(9) J. A. Connor, T. J. Meyer, and B. P. Sullivan, *Inorg. Chem.*, **18**, 1388 (1979).

(10) N. T. Albertson, *Org. React.*, **12**, 205 (1962).

(11) R. F. Lane and A. T. Hubbard, *J. Phys. Chem.*, **77**, 1401 (1973).

(12) (a) B. E. Conway, E. Gileadi, and M. Dziecivch, *Electrochim. Acta*, **8**, 143 (1963); (b) H. Angerstein-Kozlowska, J. Klinger, and B. E. Conway, *J. Electroanal. Chem.*, **75**, 45 (1977); (c) E. Laviron, *ibid.*, **52**, 395 (1974); (d) A. P. Brown and F. C. Anson, *Anal. Chem.*, **49**, 1589 (1977).

(13) J. R. Lenhard and R. W. Murray, *J. Am. Chem. Soc.*, **100**, 7870 (1978).

(14) P. J. Giordano, C. R. Bock, M. S. Wrighton, L. V. Interrante, and R. F. X. Williams, *J. Am. Chem. Soc.*, **99**, 3187 (1977).

(15) H. D. Abruña, The University of North Carolina, unpublished results.

(16) B. P. Sullivan, D. J. Salmon, and T. J. Meyer, *Inorg. Chem.*, **17**, 3334 (1978).

(17) Calculated by packing hard spheres with an average radius of 6.9 Å.

(18) D. F. Smith, K. W. Willman, K. N. Kuo, and R. W. Murray, *J. Electroanal. Chem.*, **95**, 217 (1979).

(19) C. Creutz and N. Sutin, *Proc. Natl. Acad. Sci. U.S.A.*, **72**, 2858 (1975).

(20) H. D. Abruña, G. Samuels, A. Y. Teng, and T. J. Meyer, submitted for publication.